The Journal of Neuroscience, January 15, 2000, *20*(2):529–541

A Molecular Link between Inward Rectification and Calcium Permeability of Neuronal Nicotinic Acetylcholine $\alpha3\beta4$ and $\alpha4\beta2$ Receptors

Ali Pejmun Haghighi and Ellis Cooper

Department of Physiology, McGill University, Montréal, Québec, Canada H3G 1Y6

Many nicotinic acetylcholine receptors (nAChRs) expressed by central neurons are located at presynaptic nerve terminals. These receptors have high calcium permeability and exhibit strong inward rectification, two important physiological features that enable them to facilitate transmitter release. Previously, we showed that intracellular polyamines act as gating molecules to block neuronal nAChRs in a voltage-dependent manner, leading to inward rectification. Our goal is to identify the structural determinants that underlie the block by intracellular polyamines and govern calcium permeability of neuronal nAChRs. We hypothesize that two ring-like collections of negatively charged amino acids (cytoplasmic and intermediate rings) near the intracellular mouth of the pore mediate the interaction with intracellular polyamines and also influence calcium permeability. Using site-directed mutagenesis and electrophysiology on $\alpha_4\beta_2$ and $\alpha_3\beta_4$ receptors expressed in *Xenopus* oocytes, we observed that removing the five negative charges of the cytoplasmic ring had little effect on either inward rectification or calcium permeability. However, partial removal of negative charges of the intermediate ring diminished the high-affinity, voltage-dependent interaction between intracellular polyamines and the receptor, abolishing inward rectification. In addition, these nonrectifying mutant receptors showed a drastic reduction in calcium permeability. Our results indicate that the negatively charged glutamic acid residues at the intermediate ring form both a high-affinity binding site for intracellular polyamines and a selectivity filter for inflowing calcium ions; that is, a common site links inward rectification and calcium permeability of neuronal nAChRs. Physiologically, this molecular mechanism provides insight into how presynaptic nAChRs act to influence transmitter release.

Key words: nicotinic acetylcholine receptor; presynaptic receptors; transmitter release; ion permeation; gating particles

A number of studies implicate cholinergic nicotinic receptors in a wide variety of cognitive functions, including visual and auditory processing, nociception, and attention and memory mechanisms (Piciotto et al., 1995; Bannon et al., 1998; Xiang et al., 1998; Marubio et al., 1999; Vetter et al., 1999). Many neurons express nicotinic acetylcholine receptors (nAChRs) at synapses; at some, nAChRs are located postsynaptically and mediate fast excitatory synaptic transmission, whereas at many others, nAChRs are located presynaptically and facilitate neurotransmitter release (Clarke, 1993; MacDermott et al., 1999). Functionally, neuronal nAChRs have two properties that make them suitable to influence transmitter release: they have high calcium permeability (McGehee and Role, 1995), and they inwardly rectify, that is, they conduct inward currents at negative potentials but do not conduct outward currents at positive potentials (Mathie et al., 1990; Sands and Barish, 1992; Ifune and Steinbach, 1993). Inward rectification provides an important mechanism to ensure that the receptors do not short circuit the action potential in the nerve terminal and reduce transmitter release.

That muscle nAChRs have relatively low permeability to calcium (Lewis, 1979; Adams et al., 1980) and do not show inward rectification suggests that calcium permeability and inward rectification go hand in hand for nAChRs. Interestingly, this relationship also holds for subtypes of glutamate receptors: AMPA/kainate receptors that have low calcium permeability show little inward rectification, whereas those that have high calcium permeability show strong inward rectification (Hume et al., 1991; Verdoorn et al., 1991; Dingledine et al., 1999). It is not fortuitous that these two properties correlate for AMPA/kainate receptors because the same structural determinant affects both properties. The purpose of this study is to determine the structural element or elements of neuronal nAChRs that influence calcium permeability and inward rectification.

Nicotinic AChRs have three ring-like collections of charged residues on either side of the pore (extracellular, cytoplasmic, and intermediate rings) that influence ion conduction; the intermediate ring is located at the narrowest region, or gate, of the pore and affects ion selectivity (Imoto et al., 1988; Cooper et al., 1991; Konno et al., 1991; Galzi et al., 1992; Bertrand et al., 1993; Wilson and Karlin, 1998). Previously, we demonstrated that inward rectification of neuronal nAChRs, like glutamate receptors, results from a voltage-dependent block of the receptor pore by intracellular polyamines (Haghighi and Cooper, 1998a). Our hypothesis is that the cytoplasmic and intermediate rings form the site of interaction for intracellular polyamines.

To test this hypothesis, we use a combined approach of site-directed mutagenesis of neuronal nAChR subunit cDNAs and two-electrode voltage-clamp and patch-clamp techniques on recombinant receptors expressed in Xenopus oocytes. Our results indicate that the negatively charged residues at the intermediate ring are essential for the interaction of polyamines with $\alpha4\beta2$ and

Received Aug. 30, 1999; revised Oct. 22, 1999; accepted Oct. 22, 1999.

This work was supported by the Medical Research Council of Canada. We thank L. Cooper for helpful discussions on writing scientific manuscripts.

Correspondence should be addressed to Dr. Ellis Cooper, Department of Physiology, McGill University, McIntyre Medical Building, 3655 Drummond Street, Montréal, Québec, Canada H3G 1Y6. E-Mail: ecooper@med.mcgill.ca.

$\alpha3\beta4$ neuronal nAChRs. Furthermore, we show that these negatively charged residues influence the calcium selectivity of the pore, indicating that a common structural element governs both inward rectification and calcium permeability of neuronal nAChRs.

Some of our results have been presented previously (Haghighi and Cooper, 1998b).

MATERIALS AND METHODS

Site-directed mutagenesis

We designed two complementary oligonucleotide primers containing the substituted nucleotide or nucleotides corresponding to amino acids at the cytoplasmic or intermediate ring of $\alpha3$, $\alpha4$, and $\beta4$ nAChR subunits, and used the Quick-Change Site-Directed Mutagenesis kit (Stratagene, La Jolla, CA) to mutate each subunit. Rat $\alpha3$ and $\beta4$ cDNAs were cloned into the pCDNA1 expression vector (Invitrogen, San Diego, CA), and chick $\alpha4$ and $\beta2$ (gifts from Dr. M. Ballivet, University of Geneva) were cloned into derivatives of pSV2.cat expression vectors (Cooper et al., 1991). For each reaction, we mixed 5–50 ng of the wild-type plasmid and 125 ng of each of the two primers in a solution containing 5 μl of 10× reaction buffer (Stratagene), 1 μl of dNTP mix (Stratagene), and 1 μl of pfu DNA polymerase (2.5 U/ml; Stratagene), diluted with double-distilled water to a final volume of 50 μl. The reaction mixture was then cycled in a PCR apparatus (PTC-100; MJ Research) according to the following protocol: 1 cycle at 95°C for 30 sec followed by 12–18 cycles at 95°C for 30 sec, 55°C for 1 min, and 68°C for 2 min. The following amino acids were mutated: $\alpha3$: aspartic acid (D) at position 237 to alanine (A) ($\alpha3_{D237A}$), glutamic acid (E) at position 240 to alanine ($\alpha3_{E240A}$), glutamine (Q) ($\alpha3_{E240Q}$) or aspartic acid (D) ($\alpha3_{E240D}$); $\alpha4$: glutamic acid (E) at position 242 to alanine ($\alpha4_{E242A}$) and glutamic acid at position 245 to alanine ($\alpha4_{E245A}$); $\beta4$: aspartic acid at position 236 to alanine ($\beta4_{D236A}$) and glutamic acid at position 239 to alanine ($\beta4_{E239A}$). All mutations were verified by sequencing.

Expression of nAChR subunit cDNAs in oocytes

Xenopus oocytes were defolliculated and prepared as described by Bertrand et al. (1991). We injected 1–3 ng of pairwise combinations of cDNAs coding for neuronal nAChR subunits or 3–6 ng of pairwise mutant $\alpha4$ and $\beta2$ or $\alpha3$ and $\beta4$ into the nucleus of oocytes. This difference in the amount of cDNA injection was to achieve sufficient levels of expression for the mutant receptors. Oocytes were incubated at 19°C for 2–7 d before recording. For single-channel experiments, the vitelline membrane surrounding the oocytes was removed.

Injection of BAPTA and spermine into the oocytes

To avoid the activation of the endogenous Ca^{2+}-activated Cl^- currents in the presence of extracellular Ca^{2+}, we injected oocytes 2–10 min before recording with BAPTA. The injection solution contained 100 mM BAPTA with 85 mM Na^+, 2.5 mM K^+, and 10 mM HEPES adjusted to pH 7.4 with NaOH. We injected between 30 and 60 nl of this solution into oocytes, which corresponds to a concentration of ~5–7 mM in the oocytes.

To examine the effect of the increase in the intracellular concentration of spermine on the wild-type and mutant neuronal nAChRs, we injected oocytes with 60 nl of a solution containing (in mM): 100 spermine, 100 BAPTA, 85 Na^+, 2.5 K^+, and 10 HEPES adjusted to pH 7.4. In some recordings a third electrode was used to inject spermine into the oocytes while under two-electrode clamp. In all spermine injection experiments, removal of Ca-activated Cl^- currents was used as an indication of successful injection.

Neuronal and myotube cultures

Superior cervical ganglia (SCGs) were dissected from neonatal Sprague Dawley rats (Charles River) and dissociated mechanically and enzymatically as previously described (McFarlane and Cooper, 1992). Briefly, the ganglia were dissected under sterile conditions from animals killed by cervical dislocation. The ganglia were dissociated at 37°C in collagenase (1 mg/ml, type I; Sigma, St. Louis, MO) for 15 min followed by dispase (2.4 mg/ml, grade II; Boehringer Mannheim, Indianapolis, IN) for 2–3 hr. Dissociated neurons were washed with L-15 medium supplemented with 10% horse serum and plated onto laminin-coated (40 μg/ml, overnight at 4°C; gift of Dr. S. Carbonetto, McGill University) Aclar coverslips (Allied Chemicals, Clifton, NJ) in modified Petri dishes. The neurons were incubated in 1.5 ml of L-15 medium supplemented with 5% rat serum, vitamins, cofactors, penicillin, streptomycin, and sodium bicarbonate as described previously (Hawrot and Patterson, 1979). The media was supplemented with nerve growth factor.

We used a similar method to isolate neonatal rat myoblasts. Briefly, we dissected strips of pectoral muscles from neonatal rats and dissociated them in collagenase (1 mg/ml) for 15 min at 37°C. Myoblasts were incubated in 1.5 ml of L-15 medium supplemented with 10% fetal calf serum. Myoblasts fused to form multinucleated myotubes 2–4 d after plating. All cultures were maintained at 37°C in a humidified incubator with an atmosphere of 5% CO_2 and 95% air.

Electrophysiology

Whole-cell recordings from oocytes. To measure the macroscopic ACh-evoked currents in oocytes, we used the two-electrode voltage-clamp technique (Bertrand et al., 1991). These experiments were performed at room temperature (22–24°C) using a standard voltage-clamp amplifier (built by Mr. A. Sherman, McGill University). During the recordings, oocytes were superfused with control perfusion solution or agonist solutions at 10–20 ml/min; switching from one solution to another was done manually. Recording electrodes had tip diameters of 10–15 μm and were filled with 3 M KCl. All mutant receptors, $\alpha3_{D237A}\beta4$, $\alpha3\beta4_{D236A}$, $\alpha3_{D237A}\beta4_{D236A}$, $\alpha3_{E240A}\beta4$, $\alpha3_{E240Q}\beta4$, $\alpha3_{E240D}\beta4$, $\alpha3\beta4_{E239A}$, $\alpha4_{E242A}\beta2$ and $\alpha4_{E245A}\beta2$, produced ACh-evoked currents when expressed in *Xenopus* oocytes. For equimolar injections of cDNAs, inward currents at −90 mV were on average 8–12 times smaller for the intermediate mutant receptors or 2–3 times smaller for the cytoplasmic mutant receptors compared to those for the wild-type receptors. The half-maximal concentration (EC_{50}) for ACh was not significantly different among the mutant and wild-type receptors.

To measure the current voltage (*I–V*) relationships, we used a voltage ramp protocol applied within 2–4 sec after the inward current had reached its maximum amplitude; the speed of the ramp was 333 mV/sec. Voltage ramps were applied for 360–600 msec (corresponding to 120–200 mV), during which time no significant desensitization was observed. *I–V* curves were also obtained by measuring the ACh-evoked currents at different membrane potentials (steady-state *I–V* curves). Both current and voltage traces were monitored and stored for analysis. Currents were sampled at 100–350 Hz on-line with a Pentium personal computer (PC) (running at 60 MHz and an analog-to-digital card; Omega, Stamford, CT). The program PATCHKIT (Alembic Software, Montreal, Québec, Canada) was used for stimulation and data acquisition.

External perfusion solution contained (in mM): 96 NaCl, 2 KCl, 1 $Na_2H_2PO_4$, 1 $BaCl_2$, and 10 HEPES, and 1 μM atropine; pH was adjusted with NaOH to 7.4–7.5. For Ca^{2+} permeability measurements, we used a control solution containing 1 mM $CaCl_2$ instead of $BaCl_2$ and compared the reversal potential change when we switched to a solution of either (in mM) 100 $CaCl_2$; 10 $CaCl_2$ and 90 NaCl; 25 $CaCl_2$ and 75 NaCl; or 50 $CaCl_2$ and 50 NaCl. All solutions were buffered by 10 mM HEPES and NaOH to a pH of 7.4–7.5 and contained 1 μM atropine. Spermine (Sigma) was added to the control solution containing 1 mM $BaCl_2$ where indicated. Spermine was dissolved in sterile water, and aliquots were kept frozen at −20°C.

Single-channel recordings from oocytes. Only oocytes that gave rise to large inward currents (>1 μA in response to 1 μM ACh for $\alpha4\beta2$ expressing oocytes or in response 10 μM ACh for $\alpha3\beta4$ expressing oocytes when voltage-clamped at −40 mV) were used for single-channel recordings. Outside-out recordings were performed using a List EPC-7 amplifier at room temperature (22–24°C) (Hamill et al., 1981). Pipette resistance ranged from 5 to 10 MΩ for outside-out recordings, and electrodes were coated with Sylgard (Dow Corning). Recordings were obtained in the continuous presence of ACh (0.1–0.2 μM for $\alpha4\beta2$ receptors and 1–10 μM for $\alpha3\beta4$) in the recording bath. ACh-evoked single-channel activity gradually diminished after excision of the patch (in 2–5 min). Signals were digitized with a pulse code modulation (501; Sony, Tokyo, Japan) and stored on videocassette recorder tapes. For off-line analysis, stored signals were filtered at 1.5–2 kHz with an 8-pole Bessel filter (Frequency Devices) and sampled at 10 kHz using a Pentium-60 PC. The program PATCHKIT was used for stimulation and data acquisition.

External solution contained (in mM): 100 KCl, 1 $CaCl_2$, and 10 HEPES, and 1 μM atropine, and pH was 7.4 adjusted with KOH. Recording electrodes contained (in mM): 80 KF, 20 potassium acetate, 10

HEPES, and 10 EGTA, and pH was adjusted to 7.4 with KOH. Spermine was added to the intracellular solution where indicated.

Whole-cell recordings from rat SCG neurons and cultured myotubes. Whole-cell patch-clamp recordings were performed at room temperature (22–24°C) using a List EPC-7 amplifier (Hamill et al., 1981). Throughout the recordings, cells were perfused with the external solution at a rate of 1 ml/min. ACh was applied by pressure ejection from pipettes with tip diameters of 20–30 μm (Mandelzys et al., 1995). The resistance of patch pipettes ranged from 2 to 6 MΩ, and 50–80% of the series resistance was compensated. For experiments with muscle nAChRs, we chose small multinucleated myotubes that had grown for 2–4 d in culture.

Both steady-state and ramp *I–V* curves were obtained for ACh-evoked macroscopic currents recorded from myotubes and SCG neurons. The speed of the voltage ramp protocol was 200–1000 mV/sec; voltage ramps were applied 600 msec after the application of ACh and lasted for 120–600 msec, during which time no significant desensitization was observed. Both current and voltage were monitored during the recordings and stored for analysis. Currents were filtered at 1.5 kHz with an 8-pole Bessel filter, sampled at 2.5–5 kHz, displayed and stored on-line with a Pentium-60 PC. The program PATCHKIT was used for stimulation and data acquisition.

External perfusion solution contained (in mM): 140 NaCl, 5.4 KCl, 0.33 NaH_2PO_4, 0.44 KH_2PO_4, 2.8 $CaCl_2$, 10 HEPES, 5.6 glucose, and 2 glutamine, and 0.5–1 μM TTX (Sigma) and 1 μM atropine; pH was adjusted to 7.4. Acetylcholine iodide (Ach; Sigma) was dissolved in the same external perfusion solution (100 μM for SCG neurons and 20 μM for myotubes). Recording electrodes were filled with intracellular solution containing (in mM): 70 KF, 65 potassium acetate, 5 NaCl, 1 $MgCl_2$, 10 EGTA, and 10 HEPES; pH was 7.4, adjusted with KOH.

Analysis

Whole-cell ACh-evoked *I–V* curves were obtained by subtracting the current in response to a ramp voltage change in the absence of agonist from that in the presence of agonist (Haghighi and Cooper, 1998a). The *G–V* curves were obtained by plotting the cord conductance against voltage. The cord conductance was calculated according to the following equation:

$$G = I/(V_m - E_{rev}), \quad (1)$$

where G is the cord conductance corresponding to each membrane potential (V_m), I is the ACh-evoked current at the corresponding V_m, and E_{rev} is the reversal potential.

To measure the amplitude of single-channel currents, we used either all-points histograms of open and closed distributions or measured the amplitude of the channel openings individually using PATCHKIT. Histograms were fit by Gaussian curves using Origin 4.1 graphics software (Microcal Software).

To quantify the voltage-dependent block by intracellular spermine, we fit the single-channel *G–V* relationships to a derivation of the Woodhull (1973) equation (Johnson and Ascher, 1990; Haghighi and Cooper, 1998a):

$$G/G_{max} = 1/\{1 + [S]/K_d\}, \quad (2)$$

where

$$K_d = K_{d(0)} \exp^{(-V_m z \delta F/RT)},$$

and G is the conductance in the presence of spermine at any given V_m, G_{max} is the maximum unblocked conductance, [S] is the internal concentration of spermine for outside-out patches or is the equivalent free intracellular polyamine concentration needed to produce macroscopic rectification, K_d is the dissociation constant at a given V_m, $K_{d(0)}$ is the dissociation constant at 0 mV, z is the valence of spermine, δ is the fraction of the membrane electric field sensed by spermine, and F, R, and T have their usual meanings. To estimate the intracellular concentration of spermine, we fit the macroscopic *G–V* curves to Equation 2 using the $K_{d(0)}$ and δ measured from the single-channel experiments.

To measure the effect of increasing intracellular spermine, we fit the macroscopic *G–V* curves to the Boltzmann equation:

$$G/G_{max} = 1/\{1 + (\exp^{(V - V_{1/2})/k})\}, \quad (3)$$

where $V_{1/2}$ is the membrane potential at which conductance (G) has reduced to half of the maximum conductance (G_{max}) and k is a slope factor corresponding to the amount of depolarization needed to change the conductance e-fold.

Dose–response curves for the effect of extracellular spermine were fit to a derivation of the logistic equation:

$$I/I_{max} = 1/\{1 + (IC_{50}/[S])\}, \quad (4)$$

where IC_{50} is the half-maximal inhibition dose, and [S] is the external concentration of spermine.

To calculate P_{Ca}/P_{Na}, we measured the reversal potential of the *I–V* curves in external solutions containing different amounts of Ca^{2+} and used these values in a derivation of the Goldman, Hodgkin, and Katz (GHK) constant field voltage equation as presented by Lewis (1979):

$$E_{rev(Ca)} - E_{rev(Na)} = RT/F \ln\{([Na]_o + P_K/P_{Na}[K]_o + 4P'_{Ca}/P_{Na}[Ca]_o)/ ([Na]_i + P_K/P_{Na}[K]_i + 4P'_{Ca}/P_{Na}[Ca]_i)\}, \quad (5)$$

where

$$P'_{Ca} = P_{Ca}/(1 + \exp^{(E_{rev(Ca)}F/RT)}),$$

and P_X is the permeability coefficient of ion X, $[X]_o$ is the extracellular concentration of ionic specie X, and R, T and F have their usual meanings. Concentration of each ion was multiplied by its corresponding activity coefficient (Robinson and Stokes, 1960; Butler, 1968), and P_K/P_{Na} was 1.2 (our unpublished observations). *I–V* curves were fit to a ninth order polynomial function, and reversal potentials were measured by eye. We compensated for junction potentials caused by switching between different solutions.

The best fit to the data were achieved by minimizing χ^2 using a routine from Origin 4.1 graphics software that is based on a Levenberg–Marquardt algorithm. All data points are presented as mean ± SEM. Statistical significance between values was examined using a paired Student's t test.

RESULTS

Figure 1 highlights the difference in inward rectification among nAChR subtypes. Figure 1*A* shows the ACh-evoked whole-cell current–voltage (*I–V*) relationship for native nAChRs expressed by neonatal rat sympathetic neurons from the SCG; these receptors showed strong inward rectification. Figure 1*B* shows the corresponding ACh-evoked *I–V* curve for native nAChRs expressed by neonatal rat myotubes. In contrast to nAChRs on SCG neurons, these muscle nAChRs showed little inward rectification.

To further investigate the inward rectification of neuronal nAChRs, we studied recombinant receptors in *Xenopus* oocytes. Figure 1, *C* and *D,* shows *I–V* curves for two neuronal nAChR subtypes: α4β2 receptors (Fig. 1*C*), made up of two subunits widely expressed in the CNS (Wada et al., 1989; Sargent, 1993; McGehee and Role, 1995), and α3β4 receptors (Fig. 1*D*), made up of two subunits highly expressed in peripheral autonomic neurons (Boyd et al., 1988; Couturier et al., 1990; Mandelzys et al., 1994). Similar to nAChRs on SCG neurons, the ACh-evoked *I–V* curves for both α4β2 and α3β4 receptor exhibited strong inward rectification.

Previously, we demonstrated that the strong inward rectification of α4β2 receptors results from a voltage-dependent block of the receptor pore by intracellular polyamines (Haghighi and Cooper, 1998a). A similar mechanism holds true for α3β4 receptors. Figure 1, *E* and *F*, show examples from single-channel experiments on α4β2 and α3β4 measured in outside-out patches; at positive potentials (V_m), spermine blocked the outward current from both these receptors when applied from the intracellular side. To determine the affinity of α3β4 receptors for polyamines, we repeated these single-channel experiments with four different spermine concentrations ranging from 0.1 to 100 μM on at least three different patches for each concentration and used a Woodhull (1973) model (see Materials and Methods and

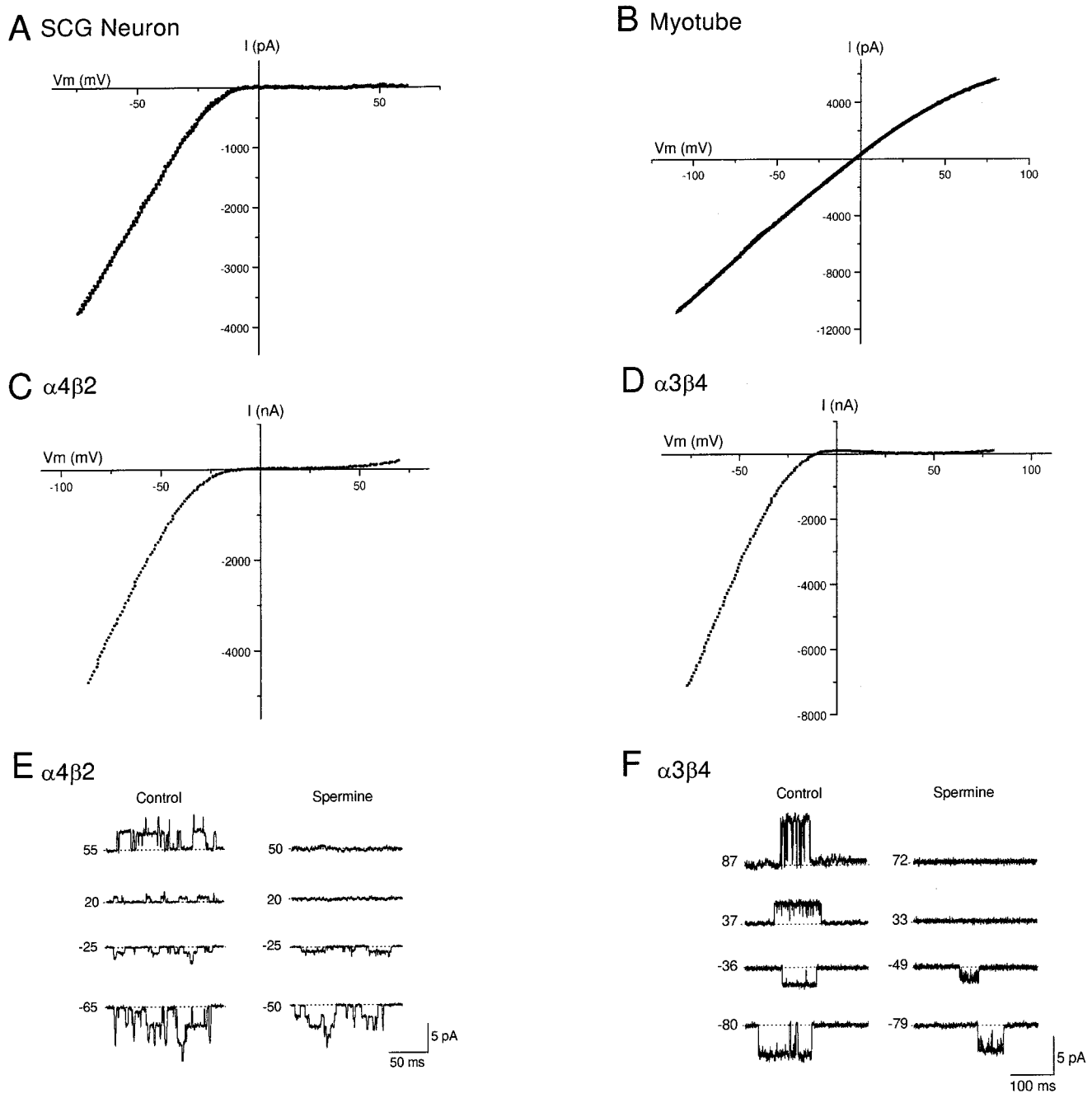

Figure 1. Inward rectification of neuronal nAChRs. *A* shows the ACh-evoked macroscopic current–voltage relationship (*I–V* curve) recorded from a neonatal rat SCG neuron. Whole-cell currents were recorded while the membrane potential was ramped from −80 to +60 mV (333 mV/sec). The *I–V* curve was obtained by subtracting the control current from the current evoked by 100 μM ACh. The *I–V* curve is fitted to a ninth order polynomial function and shows strong inward rectification. *B* shows the ACh-evoked macroscopic *I–V* curve recorded from a rat myotube (Ach, 20 μM). In contrast to *A*, this *I–V* curve shows no inward rectification. *C* shows a macroscopic ACh-evoked *I–V* curve for α4β2 neuronal nAChR, and *D* shows a macroscopic ACh-evoked *I–V* curve for α3β4 neuronal nAChR expressed in *Xenopus* oocytes. Similar to native nAChRs on SCG neurons, these recombinant receptors exhibit strong inward rectification. *E* and *F* show single-channel records obtained from outside-out patches expressing α4β2 or α3β4 receptors, respectively. In control patches, inward rectification of these receptors is lost. Addition of spermine (20 μM for α4β2 and 50 μM for α3β4) to the patch electrode blocks outward currents at positive potentials and reduces the amplitude of inward currents.

Haghighi and Cooper, 1998a) to analyze this voltage-dependent block (data not shown). From these experiments, we determined that the affinity of α3β4 receptors for spermine at 0 mV ($K_{d(0)}$) was 6.7 ± 0.5 μM, approximately twofold higher than $K_{d(0)}$ for α4β2 receptors (3.6 μM) (Haghighi and Cooper, 1998a); however, the proportion of the membrane field sensed by spermine (δ, 50–55%) was the same for both receptor types.

We were interested to determine the site of interaction between intracellular polyamines and neuronal nAChRs. Because polyamines are highly positively charged, a likely site for the interaction between neuronal nAChRs and intracellular polyamines is the negatively charged region at the cytoplasmic side of the channel pore between M1 and M2. Figure 2 shows an amino acid alignment of this region for the four neuronal nAChR

	M1	Intracellular	M2	Extracellular
α_3	VFYLPS	$_{237}$DCGEK	VTLCISVLLSLTVFLLVIT	ETIP
α_4	VFYLPS	$_{242}$ECGEK	ITLCISVLLSLTVFLLLIT	ETIP
β_2	VFYLPS	$_{236}$DCGEK	MTLCISVLLALTVFLLLIS	KIVP
β_4	VFYLPS	$_{236}$DCGEK	MTLCISVLLALTFFLLLIS	KIVP

Figure 2. Charged amino acids flanking the pore region are conserved in neuronal nAChRs subunits. This figure shows the amino acid sequence alignment of neuronal nAChR subunits $\alpha3$, $\alpha4$, $\beta2$, and $\beta4$ for the cytoplasmic end of M1, M1–M2 loop, M2 segment, and part of the M2–M3 loop. This alignment shows the presence of three ring-like accumulations of charged residues flanking M2: the cytoplasmic ring (corresponding to $\alpha3$D237), the intermediate ring (corresponding to $\alpha3$D240), and the extracellular ring (corresponding to $\alpha3$E261).

subunits: $\alpha3$, $\alpha4$, $\beta2$, and $\beta4$. The region between M1 and M2 contains five amino acids, two of which are negatively charged and are in homologous positions for each subunit. The location of the five glutamic acids (*E*), corresponding to position 240 for $\alpha3$, has been referred to as the intermediate ring, and the site of the negatively charged aspartic acid residues (*D*) ($\alpha3$, $\beta2$, and $\beta4$) or *E* ($\alpha4$) closer to M1 has been referred to as the cytoplasmic ring (Imoto et al., 1988; Galzi et al., 1991; Karlin and Akabas, 1995). We hypothesized that these negatively charged residues form the site of interaction for the positively charged polyamines. To test this, we mutated these residues to neutral amino acids, using site-directed mutagenesis, and examined the functional properties of these mutant receptors expressed in *Xenopus* oocytes.

Cytoplasmic ring mutations have little effect on inward rectification

First, we investigated the role of the cytoplasmic ring on the rectification of $\alpha3\beta4$ receptors by mutating the D at this site to alanine (*A*) for both $\alpha3$ and $\beta4$ subunits; we refer to these mutant subunits as $\alpha3_{D237A}$ and $\beta4_{D236A}$, respectively. We coexpressed pairwise combinations of mutant and wild-type $\alpha3$ and $\beta4$ cDNAs in *Xenopus* oocytes to produce three different receptors: $\alpha3_{D237A}\beta4$, $\alpha3\beta4_{D236A}$, and $\alpha3_{D237A}\beta4_{D236A}$.

For each receptor, we obtained the macroscopic ACh-evoked *I–V* curve. To quantify the rectification, we measured the relative conductance at four membrane potentials, −40 mV, +20 mV, +40 mV, and +80 mV to that at −90 mV. For $\alpha3_{D237A}\beta4$ or $\alpha3\beta4_{D236A}$ receptors, we observed no significant difference in rectification compared to that for wild-type $\alpha3\beta4$ receptors (Fig. 3*A,* Table 1). The *I–V* curves for $\alpha3_{D237A}\beta4_{D236A}$ receptors also showed strong inward rectification up to +20 mV (Fig. 3*B*); however, at V_m greater than +25 mV, we observed significantly more outward current compared to wild-type $\alpha3\beta4$ receptors. The conductance at +40 mV and that at +80 mV for $\alpha3_{D237A}\beta4_{D236A}$ receptors were approximately 12 times greater than those for wild-type $\alpha3\beta4$ receptors at these potentials.

In addition to $\alpha3\beta4$ receptors, we investigated the role of the cytoplasmic ring on the rectification of $\alpha4\beta2$ receptors. We mutated the E at 240 to A for $\alpha4$ ($\alpha4_{E242A}$) and coexpressed $\alpha4_{E242A}$ with wild-type $\beta2$ in *Xenopus* oocytes. We observed no significant difference in the ACh-evoked *I–V* curves for $\alpha4_{E242A}\beta2$ receptor compared to that for wild-type $\alpha4\beta2$ receptors (Table 1).

Removal of negative charges at the intermediate ring abolishes inward rectification

Next, we investigated the role of the intermediate ring on the rectification of $\alpha3\beta4$ receptors by mutating the E to A for both $\alpha3$ and $\beta4$ subunits; we refer to these mutant subunits as $\alpha3_{E240A}$ and $\beta4_{E239A}$, respectively. We coexpressed these mutant subunits with wild-type $\alpha3$ and $\beta4$ in *Xenopus* oocytes to produce either $\alpha3\beta4_{E239A}$ or $\alpha3_{E240A}\beta4$ receptors.

These mutations in the intermediate ring had a dramatic effect on inward rectification. Figure 3*C* shows a result from an oocyte expressing $\alpha3\beta4_{E239A}$ receptors. In contrast to wild-type $\alpha3\beta4$ receptors, the ACh-evoked *I–V* curve for $\alpha3\beta4_{E239A}$ receptors was virtually linear (Fig. 3*C*); the ACh-evoked current reversed at approximately −10 mV (Fig. 3*C*), and our ion substitution experiments indicated that this current was carried exclusively by cations (data not shown). We obtained similar results from >30 oocytes expressing $\alpha3\beta4_{E239A}$ receptors. We measured the relative conductance at −40 mV, +20 mV, +40 mV, and +80 mV to that at −90 mV (Table 1); we observed no significant difference in conductance at each potential (Table 1). The conductance at +40 mV was 93% of that at −90 mV, ~100 times greater than that of wild-type $\alpha3\beta4$ receptors.

Our results with $\alpha3\beta4_{E239A}$ receptors indicate that removal of the negative charge in the intermediate ring of $\beta4$ abolishes the strong inward rectification of $\alpha3\beta4$ receptors. To determine the effect of a similar mutation in the $\alpha3$ subunit, we examined the rectification properties of $\alpha3_{E240A}\beta4$ receptors. The ACh-evoked *I–V* curve for $\alpha3_{E240A}\beta4$ receptors was almost linear, and the current reversed at approximately −10 mV (Fig. 3*D*). The conductance at +40 mV was 79% of that at −90 mV, ~85 times greater than that of wild-type $\alpha3\beta4$ receptors (Table 1). These results indicate that removal of the negative charge in the intermediate ring of the α subunit is sufficient to abolish the strong inward rectification of $\alpha3\beta4$ receptors.

To test the effect of different amino acid side chains at the intermediate ring on rectification, we mutated E at 240 to glutamine (Q) or aspartic acid (D) in $\alpha3$ and coexpressed it with wild-type $\beta4$. The ACh-evoked *I–V* curves recorded from $\alpha3_{E240Q}\beta4$ receptors were essentially linear and not significantly different from those of $\alpha3_{E240A}\beta4$ receptors (Fig. 3*E*; Table 1). This demonstrates that neutral amino acid substitution at the intermediate ring abolishes inward rectification regardless of the side-chain size. On the other hand, $\alpha3_{E240D}\beta4$ receptors inwardly rectified, although not as strong as wild-type $\alpha3\beta4$ receptors (Table 1), indicating that the size of the negatively charged side chain influences the degree of rectification.

In addition, to test whether this effect on the rectification was specific to $\alpha3\beta4$ receptors, we mutated E at the intermediate ring to A in the $\alpha4$ subunit and coexpressed it with wild-type $\beta2$ in *Xenopus* oocytes. As shown in Figure 3*F*, these $\alpha4_{E245A}\beta2$ receptors had almost linear *I–V* curves reversing at approximately −10 mV. The conductance at +40 mV was 79% of that at −90 mV, and ~90 times greater than that of wild-type $\alpha4\beta2$ receptors (Table 1). These results demonstrate that, like $\alpha3\beta4$ receptors, partial removal of negatively charged residues in the intermediate ring abolishes strong inward rectification of $\alpha4\beta2$ receptors.

Elevated intracellular spermine increased inward rectification of $\alpha4\beta2$ and $\alpha3\beta4$ receptors, but had no effect on nonrectifying $\alpha4$E245A$\beta2$ and $\alpha3$E240A$\beta4$ receptors

Our results on intermediate ring mutations suggest that a decrease in the net negative charge of the intermediate ring abolishes the interaction of intracellular polyamines with neuronal nAChRs. To further investigate this possibility, we examined the effects of increasing the intracellular spermine concentration in *Xenopus* oocytes expressing either $\alpha4\beta2$, $\alpha3\beta4$, $\alpha4_{E245A}\beta2$, or

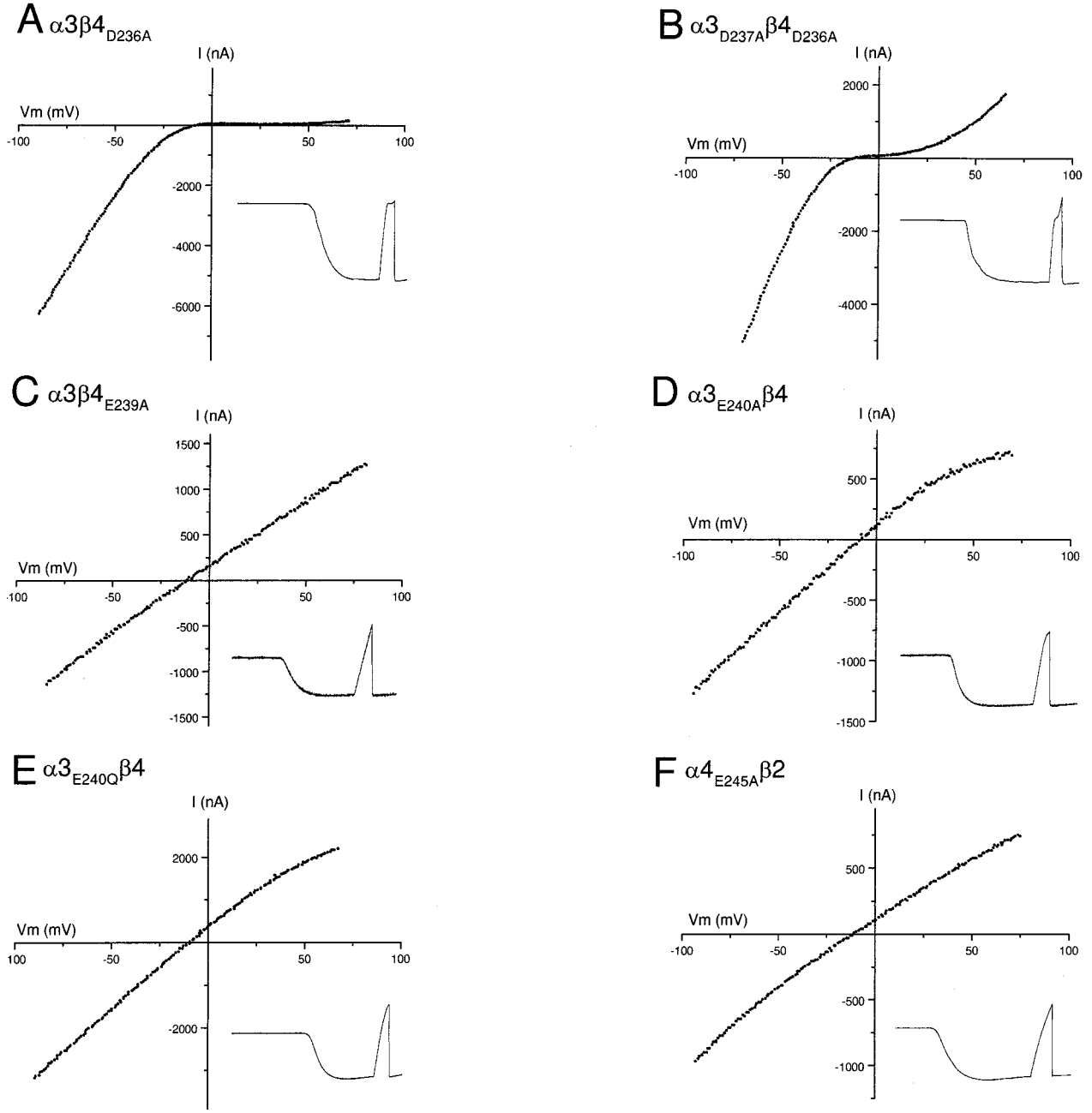

Figure 3. Substitution of negatively charged residues of the intermediate ring abolishes inward-rectification of neuronal nAChRs. *A* shows an ACh-evoked macroscopic *I–V* curve obtained from an oocyte expressing the cytoplasmic ring mutant receptor $\alpha3\beta4_{D236A}$. This mutant receptor exhibits inward rectification similar to the wild type $\alpha3\beta4$ receptor. *B* shows an ACh-evoked macroscopic *I–V* curve obtained from an oocyte expressing the cytoplasmic ring mutant receptor $\alpha3_{D237A}\beta4_{D236A}$. *C–F* show ACh-evoked macroscopic *I–V* curves obtained from oocytes expressing intermediate ring mutant receptors $\alpha3\beta4_{E239A}$, $\alpha3_{E240A}\beta4$, $\alpha3_{E240Q}\beta4$, or $\alpha4_{E245A}\beta2$. All four mutant receptors show a nearly linear ACh-evoked *I–V* relationship from −90 to +80 mV. *Insets* in each figure show ACh-evoked currents in response to a voltage ramp and demonstrate that the ACh-evoked currents do not show any significant desensitization. For all *insets* the length of the trace is 6 sec.

$\alpha3_{E240A}\beta4$ receptors. For most experiments, first we recorded the ACh-evoked *I–V* curve, then we injected the oocytes with spermine and repeated the *I–V* measurements at 2–3 min intervals. To verify that our injections worked, we included BAPTA along with spermine; in all injected oocytes, BAPTA abolished calcium-activated chloride currents when we recorded the ACh-evoked current with 1 mM Ca^{2+} as the only divalent cation in the extracellular solution (see Materials and Methods). Alone, BAPTA had no effect on inward rectification of wild-type or mutant receptors.

For ACh-evoked currents from *Xenopus* oocytes expressing wild-type $\alpha4\beta2$ or $\alpha3\beta4$ receptors, we observed that intracellular injections of spermine caused a progressive increase in rectification, producing its maximal effect in ~10 min. Figure 4 shows example *I–V* curves from $\alpha4\beta2$ (Fig. 4*A*) and $\alpha3\beta4$ (Fig. 4*D*) receptors before and after spermine injection. Increasing intracellular spermine caused a significant leftward shift in the ACh-evoked *I–V* and *G–V* curves, without affecting the ACh-evoked current amplitude at −90 mV or the reversal potential (Fig. 4). To quantify the effect of increasing intracellular spermine, we fit the

Table 1. The effect of mutations in the cytoplasmic and the intermediate ring on the macroscopic inward rectification and Ca^{2+} permeability of $\alpha4\beta2$ and $\alpha3\beta4$ nAChRs

nAChR subtype	G_{-40}/G_{-90}	G_{+20}/G_{-90}	G_{+40}/G_{-90}	G_{+80}/G_{-90}	P_{Ca}/P_{Na}	ΔE_{rev} (mV)**
$\alpha4\beta2$	31.52 ± 1.10 (n = 35)	0.42 + 0.15 (n = 35)	0.88 ± 0.22 (n = 35)	2.78 ± 0.5 (n = 33)	1.65 ± 0.15 (n = 8)	15.5 ± 1.7 (n = 8)
$\alpha4_{E242A}\beta2$	32.40 ± 2.10 (n = 6)	0.50 + 0.20 (n = 6)	1.0 ± 0.40 (n = 6)	2.50 ± 0.6 (n = 6)	N/A	N/A
$\alpha4_{E245A}\beta2$	91.6 ± 1.20* (n = 17)	81.92 ± 2.4* (n = 17)	78.7 ± 2.60* (n =17)	73.23 ± 2.9* (n = 17)	0.06 ± 0.005* (n = 6)	-40.75_1 ± 0.95* (n = 6)
$\alpha3\beta4$	44.66 ± 1.9 (n = 35)	1.75 ± 0.5 (n = 35)	0.94 ± 0.2 (n = 35)	2.06 ± 0.4 (n = 32)	0.78 ± 0.02 (n = 8)	3.6 ± 0.5 (n = 8)
$\alpha3_{D237A}\beta4$	45.8 ± 3.0 (n = 6)	1.9 ± 0.4 (n = 6)	0.64 ± 0.3 (n = 6)	2.7 ± 0.35 (n = 6)	N/A	N/A
$\alpha3\beta4_{D236A}$	45.3 ± 2.0 (n = 8)	1.76 ± 0.2 (n = 8)	0.76 ± 0.2 (n = 8)	3.76 ± 0.4 (n = 8)	N/A	N/A
$\alpha3_{D237A}\beta4_{D236A}$	49.28 ± 4.0 (n = 12)	5.75 ± 2.2 (n = 12)	11.51 ± 1.3* (n = 12)	24.42 ± 2.4* (n = 12)	0.77 ± 0.03 (n = 6)	3.30 ± 0.60 (n = 6)
$\alpha3_{E240Q}\beta4$	93.17 ± 1.7* (n = 16)	84.11 ± 2.7* (n = 16)	79.66 ± 2.7* (n = 16)	72.13 ± 3.2* (n = 16)	0.055 ± 0.007* (n = 6)	−44.2 ± 2.2* (n = 6)
$\alpha3_{E240A}\beta4$	93.78 ± 1.2* (n = 21)	82.358 ± 2.6* (n = 21)	79.30 ± 2.9* (n = 21)	75.0 ± 2.8* (n = 21)	0.062 ± 0.001* (n = 8)	−42.6 ± 2.5* (n = 8)
$\alpha3\beta4_{E239A}$	96.0 ± 1.6* (n = 31)	94.42 ± 2.6* (n = 31)	93.14 ± 2.5* (n = 31)	92.28 ± 2.6* (n = 31)	0.045 ± 0.005* (n = 6)	−47.8 ± 1.9* (n = 6)
$\alpha3_{E240D}\beta4$	97.4 ± 7.1* (n = 5)	50.2 ± 3.7* (n = 5)	41.4 ± 3.6* (n = 5)	48.2 ± 5.1* (n = 5)	N/A	N/A

*These values for mutant receptors are significantly different from those for the corresponding wild-type receptors ($p < 0.01$).
**These reversal potential shifts were measured when switching from the control solution (1 mM Ca^{2+}) to one containing 100 mM Ca^{2+}.

G–V curves to a Boltzmann equation (Eq. 3, see Materials and Methods) and determined $V_{1/2}$, the V_m where G was reduced to 50% of G_{max}, and k, the amount of depolarization needed to change the conductance e-fold. For $\alpha4\beta2$, $V_{1/2}$ was shifted to left by 16 ± 1.3 mV after spermine injection and for $\alpha3\beta4$, $V_{1/2}$ was shifted to the left by 19 ± 2.4 mV; k decreased from 14.5 ± 1.2 to 12 ± 1.5 mV for both $\alpha4\beta2$ and $\alpha3\beta4$.

To estimate the concentration of free spermine in oocytes after injection, we used the Woodhull equation (Eq. 2, see Materials and Methods). Using values for $k_{d(0)}$ and δ for $\alpha4\beta2$ (Haghighi and Cooper, 1998a) and $\alpha3\beta4$ (Fig. 1), we solved the Woodhull equation to estimate the equivalent free intracellular polyamine concentration (see Materials and Methods) [S] that best described the macroscopic *G–V* curves. The solid lines in Figure 4, *B* and *E*, represents the best fits to the Woodhull equation. Before spermine injections, [S] ranged from 70 to 80 μM in different oocytes (75.6 ± 1.6 μM; n = 37). For the oocyte expressing $\alpha4\beta2$ receptors shown in Figure 4*B*, injecting spermine increased [S] ~10-fold; for the oocyte expressing of $\alpha3\beta4$ receptors shown in Figure 4*E*, spermine injection increased [S] by ~15-fold. On average, spermine injection increased [S] by 10.1 ± 1.7-fold (n = 19). These results indicate that raising free intracellular spermine levels leads to stronger inward rectification of $\alpha4\beta2$ and $\alpha3\beta4$ receptors, providing further evidence that inward rectification of neuronal nAChRs results from a voltage-dependent block by intracellular spermine (Haghighi and Cooper, 1998a).

Next, we investigated whether increased intracellular free spermine would be sufficient to confer inward rectification to ACh-evoked currents for the intermediate ring mutant receptors. Figure 4 shows example *I–V* curves for $\alpha4_{E245A}\beta2$ (Fig. 4*C*) and $\alpha3_{E240A}\beta4$ (Fig. 4*F*) receptors before and after spermine injection. Increasing intracellular spermine caused no significant shift in the ACh-evoked *I–V* or *G–V* curves for either receptor. Furthermore, increasing intracellular spermine had no effect on the ACh-evoked current amplitudes or the reversal potential (Fig. 4*C,F*). We observed similar results from 26 of 26 oocytes. These results suggest that the reduction in the net negative charge at the intermediate ring dramatically decreases the affinity of intracellular polyamines for the receptor.

Extracellular spermine blocks nonrectifying mutant receptors

To determine whether the intermediate ring mutations affected polyamine permeability, we performed ion substitution experiments. We expressed $\alpha4_{E245A}\beta2$ receptors in *Xenopus* oocytes and then measured ACh-evoked currents in the extracellular solution containing different concentrations of spermine. With spermine as the only conducting ion in the extracellular solution, this mutant receptor failed to produce detectable ACh-evoked currents, even at −120 mV holding potential (data not shown). With an extracellular solution containing 90 mM Na^+ and 10 mM spermine, we found that spermine blocked >95% of the ACh-evoked current without affecting the reversal potential. We found that the block by extracellular spermine had little voltage dependence and reversed relatively slowly (~80% in 3–5 min). These results suggest that spermine has negligible permeability through $\alpha4_{E245A}\beta2$ receptors. To examine the block by extracellular spermine, we measured ACh-evoked currents at 3 min intervals after coapplication of 1 μM ACh with increasing concentrations of spermine. Figure 5*A* shows the spermine inhibition curves for $\alpha4\beta2$ and $\alpha4_{E245A}\beta2$ receptors; by first approximation, these curves can be described by a logistic equation (Eq. 4). From the spermine inhibition curves, we obtained the IC_{50} for mutant $\alpha4_{E245A}\beta2$ receptors (62.3 ± 13.3 μM; n = 6) and wild-type

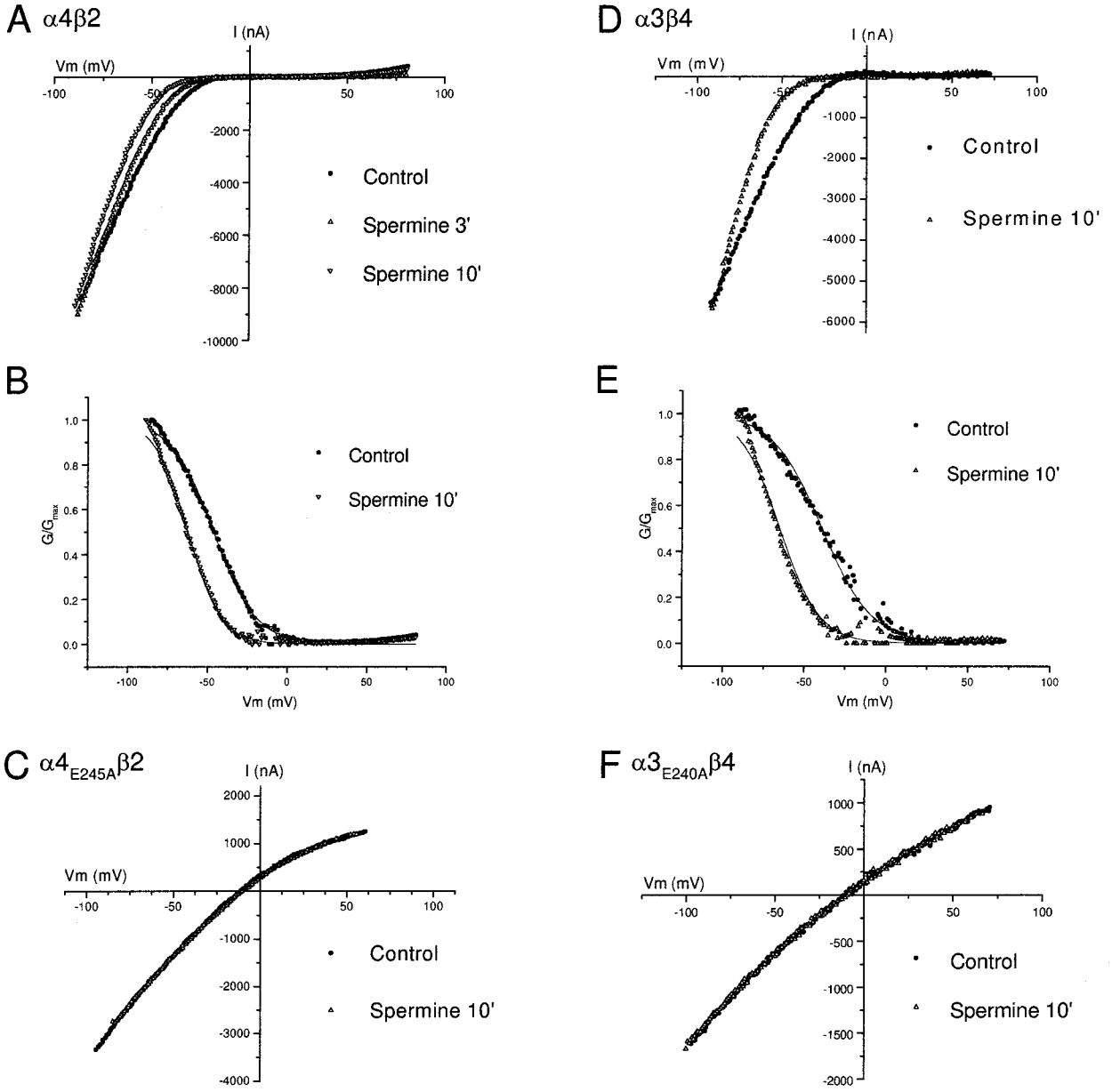

Figure 4. Effect of increasing intracellular spermine. *A* shows macroscopic ACh-evoked *I–V* curves obtained from $\alpha4\beta2$ receptors expressed in *Xenopus* oocytes. *I–V* curves were obtained before and 3 and 10 min after injecting 60 nl of a solution containing 100 mM spermine into the oocytes. *B* shows the *G–V* curves corresponding to the *I–V* curves in *A*. The *solid lines* are fits to the *G–V* curves using the Woodhull equation. The leftward shift in the *G–V* curve corresponds to an ~10-fold increase in intracellular spermine concentration. *C* shows macroscopic ACh-evoked *I–V* curves before and after injection of spermine recorded from an oocyte expressing $\alpha4_{E245A}\beta2$ receptors. There was no significant difference between the *I–V* curves before and after injection of spermine. *D* and *E* show the *I–V* and *G–V* curves from an oocyte expressing $\alpha3\beta4$ receptors before and after injection with 60 nl of a solution containing 100 mM spermine. The *solid lines* are fits to the *G–V* curves using the Woodhull equation. The leftward shift in the *G–V* curve corresponds to an ~15-fold increase in intracellular spermine concentration. *F* shows the *I–V* curves for $\alpha3_{E240A}\beta4$ receptors before and after spermine injection. Similar to $\alpha4_{E245A}\beta2$ receptors, there was no significant difference between the *I–V* curves before and after injection of spermine.

$\alpha4\beta2$ receptors (42.8 ± 5.7 μM; $n = 8$), which were not significantly different ($p > 0.05$).

We repeated these measurements on wild-type $\alpha3\beta4$ receptors and mutant $\alpha3_{E240A}\beta4$ (Fig. 5*B*). We observed no significant difference in the spermine inhibition curves between wild-type $\alpha3\beta4$ (IC_{50} = 45.1 ± 7.2 μM; $n = 5$) and mutant $\alpha3_{E240A}\beta4$ receptors (IC_{50} = 65.4 ± 12.3 μM; $n = 5$) (Fig. 5*B*). We observed similar block by extracellular spermine for $\alpha3_{E240Q}\beta4$ and $\alpha3\beta4_{E239A}$ (data not shown). The cytoplasmic ring mutant, $\alpha3_{D237A}\beta4_{D236A}$, was also blocked by extracellular spermine in a similar manner (IC_{50} = 43.8 ± 4.9 μM; $n = 5$; data not shown). These results indicate that mutations in the intermediate ring that abolish inward rectification have little effect on the block by extracellular spermine.

Relative calcium permeability

The Ca^{2+} to Na^+ permeability ratios (P_{Ca}/P_{Na}) for neuronal nAChRs have been reported to range from 0.7 to 10 depending on the subunit composition of the receptors (Sands and Barish, 1991; Adams and Nutter, 1992; Trouslard et al., 1993; Bertrand et

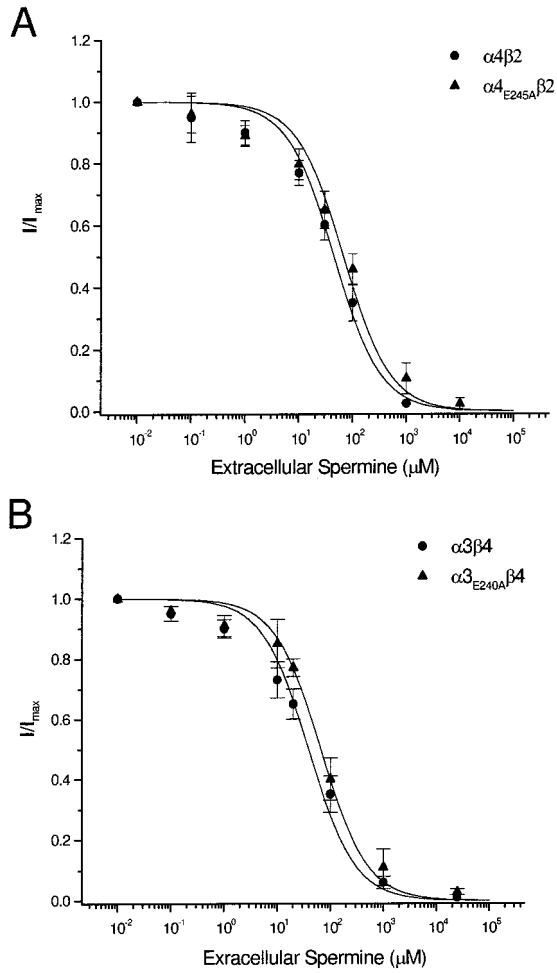

Figure 5. Extracellular spermine blocks nonrectifying mutant receptors. *A* shows the dose inhibition curves for the effect of extracellular spermine on $\alpha4\beta2$ and $\alpha4_{E245A}\beta2$, and *B* shows the dose inhibition curves for $\alpha3\beta4$ and $\alpha3_{E240A}\beta4$. Data points were fitted to a logistic equation (see Materials and Methods). There is no significant difference in the block by extracellular spermine for all four receptors.

al., 1993). Because the intermediate ring has been shown to influence permeability of cations (Konno et al., 1991; Galzi et al., 1992; Corringer et al., 1999), we compared P_{Ca}/P_{Na} among wild-type and mutant $\alpha4\beta2$ and $\alpha3\beta4$ receptors expressed in *Xenopus* oocytes. To avoid contaminating ACh-evoked currents with the endogenous Ca^{2+}-activated chloride currents in these cells (Miledi and Parker, 1984), we injected oocytes with BAPTA before our electrophysiological measurements (see Materials and Methods). In Figure 6*A*, we recorded the ACh-evoked *I–V* curve from $\alpha3\beta4$ receptors in control external solution (98 mM Na^+, 2 mM K^+, and 1 mM Ca^{2+}) and repeated the measurement in a solution containing equimolar Ca^{2+}. In 100 mM Ca^{2+}, we observed a rightward shift in the reversal potential of 3.6 mV. From the modified GHK equation (Eq. 5; Lewis, 1979; see Materials and Methods), we obtained an average P_{Ca}/P_{Na} of 0.78 ± 0.02 for $\alpha3\beta4$ receptors ($n = 8$) (Table 1). We repeated these experiments with external solutions of either 10 mM Ca^{2+} and 90 mM Na^+, 25 mM Ca^{2+} and 75 mM Na^+, or 50 mM Ca^{2+} and 50 mM Na^+. We found that P_{Ca}/P_{Na} for $\alpha3\beta4$ in all three solutions ($n = 4$ at each concentration) was not significantly different from that when we made equimolar substitutions of Na^+ and K^+ with Ca^{2+}. We observed a significant reduction of ACh-evoked currents when Ca^{2+} in the external solutions was >25 mM (Fig. 6*A*); this observation is consistent with the decrease in single-channel conductance for neuronal nAChRs when Ca^{2+} is the main charge carrier (Adams and Nutter, 1992; Mulle et al., 1992; Vernino et al., 1992).

We also measured P_{Ca}/P_{Na} for $\alpha4\beta2$ receptors (Fig. 6*B*). After switching the control external solution to 100 mM Ca^{2+}, we observed an average rightward shift in the reversal potential of 15.5 ± 0.28 mV ($n = 8$); from the GHK equation we calculated an average P_{Ca}/P_{Na} of 1.65 ± 0.15 for $\alpha4\beta2$ receptors ($n = 8$), approximately twice that for $\alpha3\beta4$ receptors (Table 1). We repeated these experiments with an external solution of 10 mM Ca^{2+} and 90 mM Na^+ and found similar values for P_{Ca}/P_{Na} ($n = 6$). Consistent with the higher value for $\alpha4\beta2$, we found that we needed to pre-inject greater amounts of BAPTA to ensure that we did not activate Ca^{2+}-activated chloride currents.

Next, we investigated whether mutations of negatively charged residues at the cytoplasmic and intermediate ring alter the relative calcium permeability of $\alpha4\beta2$ and $\alpha3\beta4$ receptors. After switching the control external solution to 100 mM Ca^{2+}, we observed a rightward shift in the reversal potential for $\alpha3_{D237A}\beta4_{D236A}$ receptors similar to that for $\alpha3\beta4$ (Fig. 6*C*, Table 1). We obtained similar results in six of six oocytes expressing $\alpha3_{D237A}\beta4_{D236A}$ receptors (Table 1). These results indicate that the negatively charged residues of the cytoplasmic ring have little influence on calcium permeability.

We tested whether mutations of charged residues at the intermediate ring alter calcium permeability by measuring P_{Ca}/P_{Na} for mutant $\alpha3_{E240A}\beta4$, $\alpha3_{E240Q}\beta4$, $\alpha3\beta4_{E239A}$, and $\alpha4_{E245A}\beta2$ receptors. Figure 6*D–F* shows example *I–V* curves for $\alpha3_{E240Q}\beta4$, $\alpha3\beta4_{E239A}$, and $\alpha4_{E245A}\beta2$ receptors with either Na^+ or Ca^{2+} as the main charge carrier. After substituting Na^+ and K^+ in the external solution with 100 mM Ca^{2+}, we observed a significant leftward shift in the *I–V* curves for all four intermediate ring mutant receptors (Table 1). Using the GHK equation (Eq. 4), we calculated that these intermediate ring mutations reduced P_{Ca}/P_{Na} by 13- to 18-fold for $\alpha3\beta4$ receptors and >25-fold for $\alpha4\beta2$ receptors (Table 1). Our results indicate that the negatively charged residues of the intermediate ring constitute a common site that governs both inward rectification and Ca^{2+} permeability of $\alpha3\beta4$ and $\alpha4\beta2$ nAChRs.

DISCUSSION

Our results add to our previous findings that strong inward rectification of neuronal nAChRs results from a voltage-dependent block by intracellular polyamines (Haghighi and Cooper, 1998a). We show that $\alpha3\beta4$ receptors have a $K_{d(0)}$ for intracellular spermine of 6.7 μM, similar to the $K_{d(0)}$ for $\alpha4\beta2$ receptors (3.6 μM). Normally, vertebrate cells have free intracellular spermine concentrations of 20–100 μM (Seiler and Schmidt-Glenewinkel, 1975; Watanabe et al., 1991; Ficker et al., 1994); this is more than sufficient to block these neuronal nAChRs. Furthermore, we show that increasing free spermine concentrations 10- to 15-fold increases this rectification by shifting the *G–V* curves toward more hyperpolarized potentials. These results provide further evidence that inward rectification of neuronal nAChRs results from a voltage-dependent block by intracellular polyamines (Haghighi and Cooper, 1998a).

We find that mutating the negatively charged glutamic acid residues of the intermediate ring to neutral amino acids removes rectification of $\alpha4\beta2$ and $\alpha3\beta4$ receptors. This is also the case for homomeric $\alpha7$ receptors (Forster and Bertrand, 1995). The *I–V*

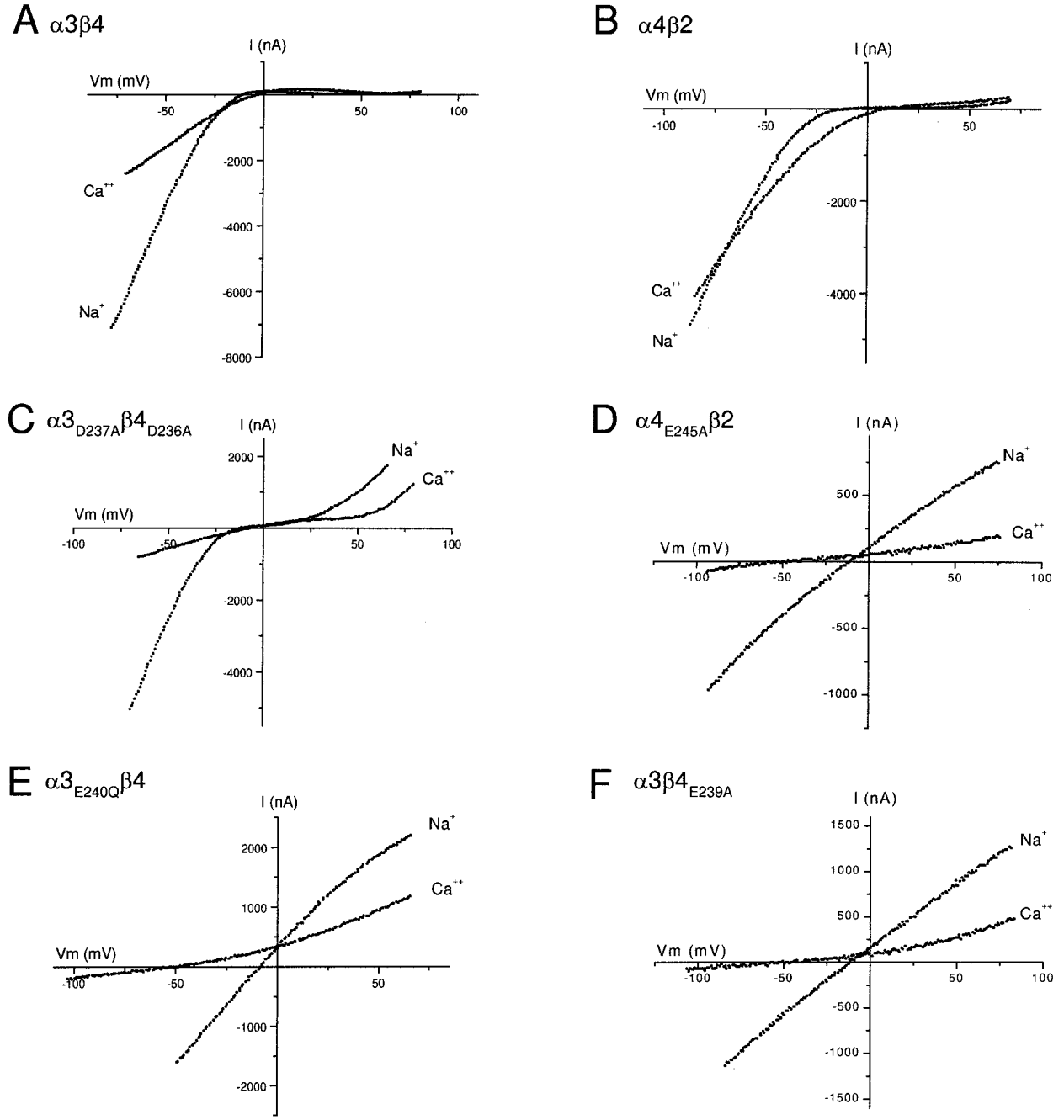

Figure 6. Substitution of the negatively charged residues of the intermediate ring with neutral amino acids drastically reduces Ca^{2+} permeability of $\alpha4\beta2$ and $\alpha3\beta4$ receptors. *A* and *B* show *I–V* curves for $\alpha3\beta4$ and $\alpha4\beta2$ receptors expressed in *Xenopus* oocytes, respectively. Switching from the control solution to one containing 100 mM Ca^{2+} causes a rightward shift of the reversal potential for both receptors. *C* shows ACh-evoked *I–V* curves for the mutant $\alpha3_{D237A}\beta4_{D236A}$ receptor in the presence of the control solution and one containing 100 mM Ca^{2+}. Switching to 100 mM Ca^{2+} causes a rightward shift of the reversal potential, similar to that observed for $\alpha3\beta4$ wild-type receptor. *D–F* shows *I–V* curves for $\alpha4_{E245A}\beta2$, $\alpha3_{E240Q}\beta4$, and $\alpha3\beta4_{E239A}$, respectively. Switching to 100 mM Ca^{2+} causes a significant leftward shift in the reversal potential for all three receptors, indicating low relative Ca^{2+} permeability for these receptors.

curves of mutant $\alpha4_{E245A}\beta2$, $\alpha3_{E240A}\beta4$, and $\alpha3\beta4_{E239A}$ receptors are essentially linear, showing very little voltage dependence. The dramatic reduction of inward rectification after alanine substitution results from the lack of charge of alanine and not from its shorter side chain length because we observed identical results with $\alpha3_{E240Q}\beta4$ receptors.

Because $\alpha4\beta2$ and $\alpha3\beta4$ receptors have pentameric structures composed of two α subunits and three β subunits (Cooper et al., 1991), we took advantage of this known subunit stoichiometry to investigate the number of negatively charged residues in the intermediate ring necessary for inward rectification. We demonstrate that mutating the negatively charged glutamic acid at the intermediate ring of either the α or the β subunit removes rectification of $\alpha4\beta2$ and $\alpha3\beta4$ receptors. Therefore, we conclude that removal of only two negative charges is sufficient to disrupt the interaction of intracellular polyamines.

Interaction between polyamines and neuronal nAChRs

To explain our results, we propose that the intermediate ring forms a high-affinity binding site for intracellular polyamines; polyamines are attracted to this site under the influence of the membrane electrical field and are held there through an electrostatic interaction with the negatively charged glutamic acids. Because the intermediate ring is at the narrowest part of the pore (Wilson and Karlin, 1998), polyamines at this site occlude the pore preventing the flow of ions.

Our model assumes that polyamines have negligible permeation through the pore. Consistent with this, our experiments on the effects of extracellular polyamines indicate that polyamines permeate the channel very poorly. We find that extracellular spermine blocks $\alpha4_{E245A}\beta2$, $\alpha3_{E240A}\beta4$, $\alpha3_{E240Q}\beta4$, and $\alpha3\beta4_{E239A}$ receptors in a similar manner to wild-type receptors. At 70–80 μM, concentrations similar to that of the cytoplasm, spermine blocks >50% of the ACh-evoked current at all membrane potentials, and at 800–1200 μM spermine blocks 80–90% of the current. This indicates that spermine has difficulty crossing the pore and likely interacts with polar and nonpolar amino acid side chains in M2 (Cui et al., 1998). If intracellular spermine could access the pore in the nonrectifying mutant receptors, we would expect it to block the channel, similar to extracellular spermine. However, even increasing intracellular spermine several fold had no effect on ACh-evoked *I–V* curve for the nonrectifying, intermediate ring mutant receptors. Therefore, it is likely that $\alpha4_{E245A}\beta2$, $\alpha3_{E240A}\beta4$, $\alpha3_{E240Q}\beta4$, and $\alpha3\beta4_{E239A}$ receptors do not rectify because the intermediate ring, with a lower net negative charge, no longer forms a high-affinity binding site for polyamines.

The region between M1 and M2 has two rings of negatively charged residues; however, the intermediate ring appears to be the major site of interaction between intracellular polyamines and the pore. Removing the negative charges at the cytoplasmic ring of either the α or β subunit has no significant effect on inward rectification. Even receptors with mutations at the cytoplasmic ring of both α and β subunits inwardly rectify, although these receptors do conduct outward current at membrane potentials greater than +25 mV; this suggests that the cytoplasmic ring also interacts with intracellular polyamines. Because spermine is approximately 20 A° long (Araneda et al., 1999) and could span both rings, we speculate that the cytoplasmic ring helps stabilize polyamines at the mouth of the pore; without these five negatively charged residues, intracellular K^+ ions destabilize the interaction of polyamines with the receptor at large depolarizations and flow out through the channel. This model has similarities to one proposed for polyamine block of AMPA receptors (Washburn et al., 1997).

Comparison to AMPA/kainate receptors

Inward rectification of calcium-permeable AMPA/kainate receptors is mediated by a voltage-dependent block by polyamines with a comparable $K_{d(0)}$ to heteromeric $\alpha4\beta2$ and $\alpha3\beta4$ nAChR (Bowie and Mayer, 1995), suggesting that the underlying mechanisms are similar. However, there are a few important differences. These AMPA/kainate receptors conduct considerable outward current at depolarized potentials (from +50 to +100 mV) (Bowie and Mayer, 1995; Koh et al., 1995), whereas we observe very little outward current from $\alpha4\beta2$ and $\alpha3\beta4$ receptors at these potentials. Furthermore, nonrectifying AMPA/kainate receptors, whose subunits have undergone RNA editing substituting a glutamine (Q) to an arginine (R) in the pore region, are not blocked by extracellular spermine (Washburn and Dingledine, 1996; Bähring et al., 1997; Washburn et al., 1997); in contrast, extracellular spermine blocks nonrectifying mutant $\alpha4\beta2$ and $\alpha3\beta4$ receptors. These differences may be explained, in part, by differences in the putative location of the high-affinity polyamine binding-site in the pore. For AMPA/kainate receptors, this site appears to be near the middle of the pore (Kuner et al., 1996; Washburn et al., 1997), whereas for neuronal nAChRs, this site is most likely at the cytoplasmic mouth of the pore (Imoto et al., 1988; Wilson and Karlin, 1998). The high-affinity polyamine site in rectifying AMPA/kainate receptors is formed the by a ring of glutamine residues as well as by negatively charged aspartate or glutamate residues four amino acids downstream (Washburn et al., 1997). Similarly, the high-affinity polyamine site in neuronal nAChRs is formed the by the intermediate and cytoplasmic rings, which are four amino acids apart. Interestingly, substituting two glutamic acid residues with glutamines at the intermediate ring of neuronal nAChRs abolishes inward rectification, suggesting that the geometry of the high-affinity polyamine site in AMPA/kainate receptors and neuronal nAChRs is different.

A common site affects both inward rectification and calcium permeability

For AMPA/kainate receptors, there is a strong correlation between calcium permeability and inward rectification (Verdoorn et al., 1991; Hume et al., 1991; Dingledine et al., 1999). This correlation holds true for nAChRs as well. Muscle nAChRs, which rectify slightly, have low calcium permeability (Adams et al., 1980; Villarroel and Sakmann, 1996), whereas neuronal nAChRs, which show strong inward rectification, have high calcium permeability (McGehee and Role, 1995). Calcium permeability of nAChRs appears to be influenced by residues in the M2 as well as residues in the intermediate ring (Bertrand et al., 1993; Villarroel and Sakmann, 1996). Our results on relative calcium permeability for $\alpha4\beta2$ and $\alpha3\beta4$ receptors are consistent with this. Our ion substitution experiments indicate that P_{Ca}/P_{Na} is 1.65 for $\alpha4\beta2$ receptors and 0.8 for $\alpha3\beta4$ receptors; the amino acid differences in the M2 between these receptors likely underlie the differences in Ca^{2+} permeability.

In addition, we show that partial removal of negative charges in the intermediate ring reduces P_{Ca}/P_{Na} by ~15-fold for $\alpha3\beta4$ and 25-fold for $\alpha4\beta2$ receptors. We observe similar reduction in P_{Ca}/P_{Na} when we substitute glutamic acid residues by either alanine or glutamine residues in the intermediate ring; this indicates that the reduction in calcium permeability is caused by a change in net negative charge of the intermediate ring and not by alteration in the size or polarity of the amino acid side chains. We find that substituting all five negatively charged residues with neutral residues at the cytoplasmic ring has no effect on P_{Ca}/P_{Na}, further demonstrating the important role of the intermediate ring in determining calcium permeability. Therefore, a common structural element of neuronal nAChRs governs both interaction with intracellular polyamines and high calcium permeability.

Physiological implications

In the CNS, many neuronal nAChRs are located at presynaptic nerve terminals (MacDermott et al., 1999). Given the small size and high input impedance of nerve terminals together with the relatively large single-channel conductance of neuronal nAChRs, activation of only a few nAChRs would likely trigger action potentials in the terminal and evoke transmitter release. Support for this idea comes from studies on adrenal chromaffin cells in

which activation of a single nAChR is sufficient to evoke action potentials (Fenwick et al., 1982). In the absence of inward rectification, the ACh-evoked conductance in the terminal would act to shunt the action potential, preventing it from reaching its full amplitude. Considering the steep relationship between presynaptic depolarization and transmitter release, a reduction in action potential amplitude in the terminal would severely affect release. To ensure that the action potential reaches its full amplitude, intracellular polyamines rapidly block neuronal nAChRs by interacting with the intermediate ring in a voltage-dependent manner.

In this study, we provide a molecular understanding of inward rectification of neuronal nAChRs and establish a link between two important physiological properties of these receptors, calcium permeability and inward rectification. By linking these two properties through a common structural element, neuronal nAChRs limit the inflow of calcium into the cell, thereby preventing excitotoxicity. Equally important, small depolarizations from rest can lead to screening of the negative charges at the intermediate ring by intracellular polyamines, thereby modulating calcium inflow through these receptors.

REFERENCES

Adams DJ, Nutter TJ (1992) Calcium permeability and modulation of nicotinic acetylcholine receptor-channels in rat parasympathetic neurons. J Physiol (Lond) 86:67–76.

Adams DJ, Dwyer TM, Hille B (1980) The permeability of endplate channels in monovalent and divalent metal cations. J Gen Physiol 75:493–510.

Araneda R, Lan JY, Zheng X, Zukin S, Bennett VL (1999) Spermine and arcaine block and permeate *N*-methyl-D-aspartate receptor channels. Biophys J 76:2899–2911.

Bähring R, Bowie D, Benveniste M, Mayer ML (1997) Permeation and block of rat GluR6 glutamate receptor channels by internal and external polyamines. J Physiol (Lond) 502:575–589.

Bannon AW, Decker MW, Holladay MW, Curzon P, Donnelly-Roberts D, Puttfarcken PS, Bitner RS, Diaz A, Dickenson AH, Porsolt RD, Williams M, Arneric SP (1998) Broad-spectrum, non-opioid analgesic activity by selective modulation of neuronal nicotinic acetylcholine receptors. Science 279:77–81.

Bertrand D, Cooper E, Valera S, Rungger D, Ballivet M (1991) Electrophysiology of neuronal nicotinic acetylcholine receptors expressed in *Xenopus* oocytes following nuclear injection of genes or cDNAs. Methods Neurosci 4:174–193.

Bertrand D, Galzi JL, Devillers-Thiéry A, Bertrand S, Changeux JP (1993) Mutations at two distinct sites within the channel domain M2 alter calcium permeability of neuronal a7 nicotinic receptor. Proc Natl Acad Sci USA 90:6971–6975.

Bowie D, Mayer ML (1995) Inward rectification of both AMPA and kainate subtype glutamate receptors generated by polyamine-mediated ion channel block. Neuron 15:453–462.

Boyd RT, Jacob MH, Couturier S, Ballivet M, Berg DK (1988) Expression and regulation of neuronal acetylcholine receptor mRNA in chick ciliary ganglia. Neuron 1:495–502.

Butler JN (1968) The thermodynamic activity of calcium ion in sodium chloride-calcium chloride electrolytes. Biophys J 8:1426–1433.

Clarke PBS (1993) Nocotinic receptors in mammalian brain: localization and relation to cholinergic innervation. Prog Brain Res 98:77–83.

Cooper E, Couturier S, Ballivet M (1991) Pentameric structure and subunit stoichiometry of a neuronal nicotinic acetylcholine receptor. Nature 350:235–238.

Corringer PJ, Bertrand S, Galzi JL, Devillers-Thiery A, Changeux JP, Bertrand D (1999) Mutational analysis of the charge selectivity filter of the α7 nicotinic acetylcholine receptor. Neuron 22:831–843.

Couturier S, Erkman L, Valera S, Rungger D, Bertrand S, Boulter J, Ballivet M, Bertrand D (1990) α_5, α_3 and non- α_3: three clustered avian genes encoding neuronal nicotinic acetylcholine receptor-related subunits. J Biol Chem 265:17560–17567.

Cui C, Bähring R, Mayer ML (1998) The role of hydrophobic interactions in binding of polyamines to non NMDA receptor ion channels. Neuropharmacology 37:1381–1391.

Dingledine R, Borges K, Bowie D, Traynelis SF (1999) The glutamate receptor ion channels. Pharmacol Rev 51:7–61.

Fenwick E, Marty A, Neher E (1982) A patch-clamp study of bovine chromaffin cells and of their sensitivity to acetylcholine. J Physiol (Lond) 331:577–597.

Ficker E, Taglialatela M, Wible BA, Henley CM, Brown AM (1994) Spermine and spermidine as gating molecules for inward rectifier K^+ channels. Science 266:1068–1072.

Forster I, Bertrand D (1995) Inward rectification of neuronal nicotinic acetylcholine receptors investigated by using the homomeric α7 receptor. Proc R Soc Lond B Biol Sci 260:139–148.

Galzi JL, Revah F, Bessis A, Changeux JP (1991) Functional architecture of the nicotinic acetylcholine receptor: from electric organ to brain. Annu Rev Pharmacol 31:37–72.

Galzi JL, Devillers-Thiery A, Hussy N, Bertrand S, Changeux JP, Bertrand D (1992) Mutations in the channel domain of a neuronal nicotinic receptor convert ion selectivity from cationic to anionic. Nature 359:500–505.

Haghighi AP, Cooper E (1998a) Neuronal nicotinic acetylcholine receptors are blocked by intracellular spermine in a voltage-dependent manner. J Neurosci 18:4050–4062.

Haghighi AP, Cooper E (1998b) Neuronal nicotinic acetylcholine receptors inwardly rectify through an interaction between intracellular polyamines and negatively charged residues on the cytoplasmic side of the pore. Soc Neurosci Abstr V24:1340.

Hamill OP, Marty A, Neher E, Sakmann B, Sigworth F (1981) Improved patch clamp techniques for high resolution current recording from cells and cell-free membrane patches. Pflügers Arch 391:85–100.

Hawrot E, Patterson P (1979) Long-term culture of dissociated sympathetic neurons. Methods Enzymol 58:574–584.

Hume RI, Dingledine R, Heinemann SF (1991) Identification of a site in glutamate receptor subunits that controls calcium permeability. Science 253:1028–1031.

Ifune CK, Steinbach JH (1993) Modulation of acetylcholine-elicited currents in clonal rat phaeochromocytoma (PC12) cells by internal polyphosphates. J Physiol (Lond) 463:431–447.

Imoto K, Busch C, Sakmann B, Mishina M, Konno T, Nakai J, Bujo H, Mori Y, Fukuda K, Numa S (1988) Rings of negatively charged amino acids determine the acetylcholine receptor channel conductance. Nature 335:645–648.

Johnson JW, Ascher P (1990) Voltage-dependent block by intracellular Mg^{++} of *N*-methyl-D-aspartate-activated channels. Biophys J 57:1085–1090.

Karlin A, Akabas MH (1995) Toward a structural basis for the function of nicotinic acetylcholine receptors and their cousins. Neuron 15:1231–1244.

Koh DS, Burnashev N, Jonas P (1995) Block of native Ca2+-permeable AMPA receptors in rat brain by intracellular polyamines generates double rectification. J Physiol (Lond) 486:305–312.

Konno T, Busch C, Von Kitzing E, Imoto K, Wang F, Nakai J, Mishina M, Numa S, Sakmann B (1991) Rings of anionic amino acids as structural determinants of ion selectivity in the acetylcholine receptor channel. Proc R Soc Lond B Biol Sci 244:69–79.

Kuner T, Wollmuth LP, Karlin A, Seeburg PH, Sakmann B (1996) Structure of the NMDA receptor channel M2 segment inferred from the accessibility of substituted cysteines. Neuron 17:343–352.

Lewis CA (1979) Ion-concentration dependence of the reversal potential and the single channel conductance of ion channels at the frog neuromuscular junction. J Physiol (Lond) 286:417–445.

Mandelzys A, Pie B, Deneris ES, Cooper E (1994) The developmental increase in ACh current densities on rat sympathetic neurons correlates with changes in nicotinic ACh receptor a-subunit gene expression and occurs independent of innervation. J Neurosci 14:2357–2364.

Mandelzys A, De Koninck P, Cooper E (1995) Agonist and toxin sensitivities of ACh-evoked currents on neurons expressing multiple nicotinic ACh receptor subunits. J Neurophysiol 74:1212–1221.

Marubio LM, Del-Mar-Arroyo-Jimenez M, Cordero-Erausquin M, Léna C, LeNovèrre N, De Kerchove d'Exaerde A, Huchet M, Damaj I, Changeux JP (1999) Reduced antinociception in mice lacking neuronal nicotinic receptor subunits. Nature 398:805–810.

Mathie A, Colquhoun D, Cull-Candy SG (1990) Rectification of currents activated by nicotinic acetylcholine receptors in rat sympathetic ganglion neurons. J Physiol (Lond) 427:625–655.

MacDermott AB, Role LW, Siegelbaum D (1999) Presynaptic iono-

tropic receptors and the control of transmitter release. Annu Rev Neurosci 22:443–485.
McFarlane S, Cooper E (1992) Postnatal development of voltage-gated K currents on rat sympathetic neurons. J Neurosci 67:1291–1300.
McGehee DS, Role LW (1995) Physiological diversity of nicotinic acethylcholine receptors expressed by vertebrate neurons. Annu Rev Physiol 57:521–546.
Miledi R, Parker I (1984) Chloride currents induced by injection of Ca^{++} into *Xenopus* oocytes. J Physiol (Lond) 357:173–183.
Mulle C, Léna C, Changeux JP (1992) Potentiation of nicotinic receptor response by external calcium in rat central neurons. Neuron 8:937–945.
Picciotto MR, Zoll M, Léna C, Bessis A, Lallemand Y, LeNovèrre N, Vincent P, Pich EM, Brulet P, Changeux JP (1995) Abnormal avoidance learning in mice lacking functional high-affinity nicotine receptor in the brain. Nature 374:65–67.
Robinson RA, Stokes RH (1960) Electrolyte solutions. London: Butterworths Scientific Publication.
Sands SB, Barish ME (1991) Calcium permeability of neuronal nicotinic acetylcholine receptor channels in PC12 cells. Brain Res 560:38–42.
Sands SB, Barish ME (1992) Neuronal nicotinic acetylcholine receptor currents in phaeochromocytoma (PC12) cells: dual mechanisms of rectification. J Physiol (Lond) 447:467–487.
Sargent PB (1993) The diversity of neuronal nicotinic acetylcholine receptors. Annu Rev Neurosci 16:403–443.
Seiler N, Schmidt-Glenewinkel T (1975) Regional distribution of putrescine, spermidine and spermine in relation to the distribution of RNA and DNA in the rat nervous system. J Neurochem 24:791–795.
Trouslard J, Marsh SJ, Brown DA (1993) Calcium entry through nicotinic receptor channels and calcium channels in cultured rat superior cervical ganglion cells. J Physiol (Lond) 468:53–71.
Vetter DE, Liberman MC, Mann J, Barhanin J, Boulter J, Brown MC, Saffiote-Kolman J, Heinemann SF, Elgohhen AB (1999) Role of alpha 9 nicotinic ACh receptor subunits in the development and function of cochlear efferent innervation. Neuron 23:93–103.
Verdoorn TA, Burnashev N, Monyer H, Seeburg PH, Sakmann B (1991) Structural determinants of ion flow through recombinant glutamate receptor channels. Science 252:1715–1718.
Vernino S, Amador M, Luetje CW, Patrick J, Dani JA (1992) Calcium modulation and high calcium permeability of neuronal nicotinic acetylcholine receptors. Neuron 8:127–134.
Villarroel A, Sakmann B (1996) Calcium permeability increase of endplate channels in rat muscle during postnatal development. J Physiol (Lond) 496:331–338.
Wada E, Wada K, Boulter J, Deneris E, Heinemann S, Patrick J, Swanson LW (1989) Distribution of α_2, α_3, α_4, and β_2 neuronal nicotinic receptor subunit mRNA in the central nervous system: a hybridization histochemical study in the rat. J Comp Neurol 284:314–335.
Washburn MS, Dingledine R (1996) Block of α-amino-3-hydroxy-5-methyl-4-isoxazolepropionic acid (AMPA receptors by polyamines and polyamine toxins. J Pharmacol Exp Ther 278:669–678.
Washburn MS, Numberger M, Zhang S, Dingledine R (1997) Differential dependence on GluR2 expression of three characteristic features on AMPA receptors. J Neurosci 17:9393–9406.
Watanabe S, Kusama-Eguchi K, Kobayashi H, Igarashi K (1991) Estimation of polyamine binding to macromolecules at ATP in bovine lymphocytes and rat liver. J Biol Chem 266:20803–20809.
Wilson GG, Karlin A (1998) The location of the gate in the acetylcholine receptor. Neuron 20:1269–1281.
Woodhull AM (1973) Ionic blockage of sodium channels in nerve. J Gen Physiol 61:687–708.
Xiang Z, Hunguenard JR, Prince DA (1998) Cholinergic switching within neocortical inhibitory networks. Science 281:985–988.